Published in "European Journal of Neuroscience 50(4): 2694–2706, 2019"
which should be cited to refer to this work.

Inducible and reversible silencing of the *Pvalb* gene in mice: An in vitro and in vivo study

Federica Filice | **Walter Blum** | **Emanuel Lauber** | **Beat Schwaller**

Department of Neuroscience & Movements Science, Section of Medicine, University of Fribourg, Fribourg, Switzerland

Correspondence
Beat Schwaller, Department of Neuroscience & Movements Science, Section of Medicine, University of Fribourg, Fribourg, Switzerland.
Email: beat.schwaller@unifr.ch

Present address
Walter Blum, Genetica AG, Weinbergstrasse 9, Zurich, CH-8001, Switzerland

Funding information
Schweizerischer Nationalfonds zur Förderung der Wissenschaftlichen Forschung, Grant/Award Number: 310030_155952/1; Novartis Stiftung für Medizinisch-Biologische Forschung, Grant/Award Number: 16C172

Abstract

Inducible and reversible regulation of gene expression is a powerful approach for unraveling gene functions. Here, we describe the generation of a system to efficiently downregulate in a reversible and inducible manner the *Pvalb* gene coding for the calcium-binding protein parvalbumin (PV) in mice. We made use of an IPTG-inducible short hairpin RNA to activate *Pvalb* transcript knockdown and subsequently downregulate PV. The downregulation was rapidly reversed after withdrawal of IPTG. In vitro and in vivo experiments revealed a decrease in PV expression of ≥50% in the presence of IPTG and full reversibility after IPTG removal. We foresee that the tightly regulated and reversible PV downregulation in mice in vivo will provide a new tool for the control of *Pvalb* transcript expression in a temporal manner. Because PV protein and *PVALB* transcript levels were found to be lower in the brain of patients with autism spectrum disorder and schizophrenia, the novel transgenic mouse line might serve as a model to investigate the putative role of PV in these neurodevelopmental disorders.

KEYWORDS
inducible system autism spectrum disorder, lentiviral transgenesis, parvalbumin, RNA interference

1 | INTRODUCTION

For decades, mouse models are considered as powerful research tools, due to the genome similarity they share with humans (Yue et al., 2014) and the possibility to correlate results from mouse experiments to human biology. Furthermore, the mouse genome is easily accessible to manipulation and since 1974 (Jaenisch & Mintz, 1974), the number of transgenic mouse lines carrying mutations that lead to a gain- or loss-of-function for a specific gene is constantly increasing.

The subpopulation of PV-immunoreactive (PV^+) neurons, hereafter called Pvalb neurons (irrespective of PV expression levels), have become very popular in the last few years due to their emerging role in neuropsychiatric disorders such as schizophrenia and autism spectrum disorder (ASD) (Ferguson & Gao, 2018; Marin, 2012). The study of Pvalb neurons is facilitated by the availability of several transgenic mouse lines; up to date, fluorescent protein expression such as GFP or RFP have been targeted to Pvalb neurons to facilitate their direct identification (Kaiser, Ting, Monteiro, & Feng, 2016; Meyer, Katona, Blatow, Rozov, & Monyer, 2002); in addition, mouse lines expressing the Cre-recombinase (Hippenmeyer et al., 2005) selectively in Pvalb neurons, as well as PV-knockout ($PV^{-/-}$) mice (Schwaller et al., 1999) are available from common repositories.

Nevertheless, studying PV function in mice is still challenging. The difficulty is based on the fact that, despite the availability of knockout models and/or Cre-expressing lines, a temporal-inducible and reversible control of the *Pvalb* gene expression is still missing. Here, we report a method for *Pvalb*

Edited by Paul Bolam. Reviewed by Patricia Gaspar and Tibor Harkany.

All peer review communications can be found with the online version of the article.

transcript knockdown in an inducible and reversible manner, combining the use of short hairpin RNA and lentiviral-mediated transgenesis. We provide evidence for the efficacy of our system in vitro, in ex vivo fibroblasts isolated from mice carrying the transgene and finally, present proof-of-principle data that reversible *Pvalb* regulation is also occurring in transgenic mice in vivo.

2 | METHODS AND MATERIALS

2.1 | Generation of Phage2-PV and Short hairpin RNAs

The plasmids for lentivirus (LV) production were obtained from Addgene and included Phage2–Cre reporter (plasmid #62732 (D'Astolfo et al., 2015)), mRFP1-C1 coding for monomeric red fluorescent protein (Plasmid #54764 (Campbell et al., 2002)), envelope vector pMD2.G-VSVG, and packaging vector psPAX2 (gift from Didier Trono, plasmids #12259 and #12260, respectively). Briefly, the rat *Pvalb* coding sequence (CDS) was cloned into Phage2 using the NotI and BamHI sites. *Pvalb* CDS (330 bp) was amplified from the pCMV-PV plasmid (D'Orlando et al., 2001) using the primers NotI-PV (5′-AGTC*GCGGCCGC*ATGTCG ATGACAGACTT-3′) and BamHI (5′-AGTC*GGATCC* TTAGCTTTCGGCCACCAGAGT-3′) and inserted into the Phage2 vector to produce the final lentiviral plasmid named Phage2-PV. A Phage2-mRFP-PV LV was also created to visualize PV distribution in live cells, more precisely of the fusion protein RFP-PV. *Pvalb* CDS was first subcloned into the mRFP-C1 plasmid using SalI (5′-ATCA*GTCGAC*TCGATGACAGACTTGCTC) and BamHI (5′-AGTC*GGATCC*TTAGCTTTCGGCCACCAG AGT) sites. Then, the mRFP-PV insert was cloned into the Phage2 vector as described above.

The Isopropyl-β-D-thio-galactoside (IPTG)-inducible LV-shRNA plasmid coding for shRNA against mouse *Pvalb* named 3X-LacO-pLKO.1-shPV22 (named according to the last two digits of The RNAi Consortium number TRCN0000104822) was purchased from Sigma-Aldrich, Buchs, Switzerland. An IPTG-inducible shRNA plasmid coding for shRNA against Turbo-GFP and not complementary to any mouse sequence was used as control. To facilitate the identification of cells transfected with the shRNAs both in vitro and in vivo, the puromycin resistance cassette was replaced with the one coding for the enhanced green fluorescent protein (eGFP), using BamHI and SbfI sites. Plasmid maps of the inducible vectors are depicted in Figure 1. The eGFP plasmid was obtained from Prof. Trono's lab (EPFL, Lausanne, Switzerland). All plasmids were verified by DNA sequencing.

2.2 | Lentiviral production, cell transduction and in vitro tests

Lentiviral vectors for in vitro experiments were produced in HEK293T cells according to the protocol described before

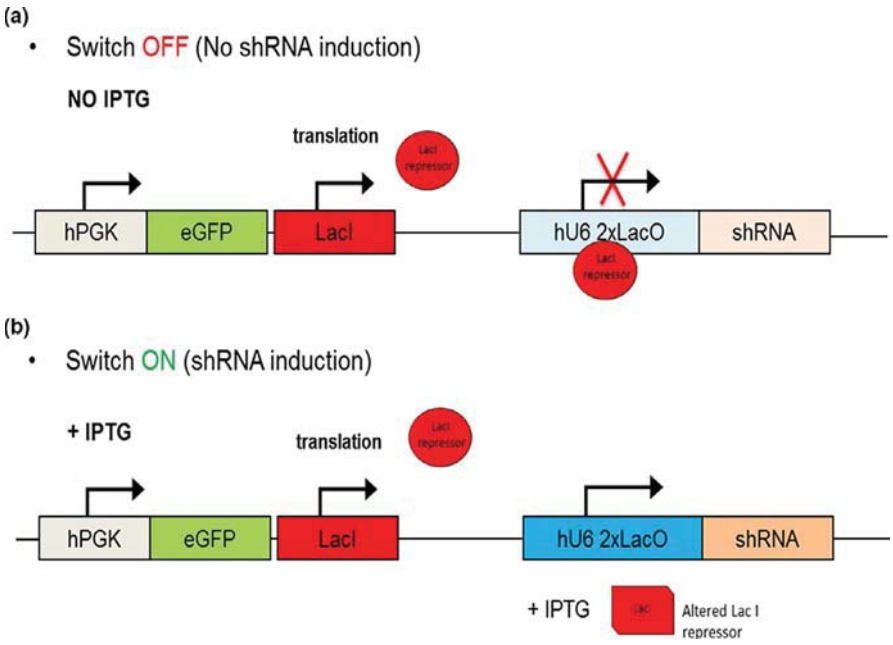

FIGURE 1 Schematic representation of the genetic system used to achieve inducible and reversible shRNA expression in vitro and in vivo. (a) The IPTG-inducible vector contains *lac* operon (LacO) sequences responsible for tight regulation and gene silencing. In the absence of IPTG, the LacI repressor binds to LacO preventing the expression of the shRNA. (b) In the presence of IPTG, the LacI repressor changes conformation, releasing itself from the LacO sites of the modified human U6 promoter and subsequently allowing for the expression of the *Pvalb* or *TurboGFP* shRNA. eGFP, enhanced green fluorescent protein; shRNA, short hairpin RNA. [Colour figure can be viewed at wileyonlinelibrary.com]

(Kutner, Zhang, & Reiser, 2009). Briefly, the plasmids carrying transgene sequences (see above), the envelope vector pMD2.G-VSVG and the packaging vector psPAX2 (ratio 10:3:8 μg) were co-transfected in HEK293T cells. LV-containing medium was collected 48 and 72 hr after transfection and filtered through 0.45 μm polyethersulfone (PES) filters, then aliquoted and stored at −80°C.

Murine RN5 mesothelioma cells isolated as described before (Blum et al., 2015) or isolated primary mouse lung fibroblasts (Seluanov, Vaidya, & Gorbunova, 2010) (see below), cultured in DMEM (GIBCO, Basel, Switzerland) supplemented with 10% fetal bovine serum (FBS; Gibco) and 100 U/ml penicillin and 100 μg/ml streptomycin (1% PS; Gibco), were used for the in vitro/ex vivo experiments, respectively. RN5 cells were seeded in six-well plates and cotransduced with Phage2-PV resulting in cells hereafter named RN5-PV cells containing either one of two different inducible lentiviral constructs: 3X-LacO-eGFP-shPV22, 3X-LacO-eGFP-shTurboGFP (negative control). Primary mouse lung fibroblasts from transgenic mice (lines: 277_F3 and 284_F3, see below) were transduced with Phage2-PV or Phage2-mRFP-PV.

Cell growth (confluence) and green fluorescence were monitored by the Incucyte Live Cell Imaging System™ (Essen Bioscience, Michigan). Isopropyl-β-D-thio-galactoside (IPTG; 1 mM; Sigma-Aldrich) was added to the culture medium of both RN5 cells and fibroblasts after eGFP expression was detectable by the Incucyte Imaging system. Medium containing fresh IPTG (1 mM) was changed every 2–3 days; IPTG did not affect cell growth (data not shown). RN5-PV cells were harvested day by day for five consecutive days. On the fifth day of harvesting, part of the cells were split and kept in culture in medium without IPTG and collected day by day for 5 days. PV downregulation and PV re-expression were analyzed by western blot and RT-qPCR analyses. Primary mouse lung fibroblasts were cultured in the presence of IPTG for 7 days; PV downregulation was analyzed by western blot.

2.3 | Generation of the mouse line B6PV^{Cre}-Tg(hPGK-eGFP/Rnai; Pvalb)^{1Swal}

All experiments were performed with permission of the local animal care committee (Canton of Fribourg, Switzerland) and according to the present Swiss law and the European Communities Council Directive of 24 November 1986 (86/609/EEC). B6.129P2-Pvalb$^{tm1(cre)Arbr}$/J mice, also known as PV-Cre mice (Hippenmeyer et al., 2005), were housed in temperature-controlled animal facilities (24°C, 12:12 hr light/dark cycle), at the University of Fribourg, Switzerland and fed ad libitum. Three-week-old female mice and competent male breeders were sent to the Transgenic Core Facilities of EPFL, Lausanne, Switzerland, where the lentiviral transgenesis in vivo was performed according to the protocol described in Barde, Verp, Offner, & Trono, (2011). As the efficiency of transgenesis strongly depends on the quality and titer of the lentiviral vectors, 3X-LacO-eGFP-shPV22 and 3X-LacO-eGFP-shTurboGFP vectors for the in vivo experiments were produced and purified at the transgenic core facilities of EPFL, as described previously (Barde, Salmon, & Trono, 2010). Transgenic mice were generated by injection of LV into the perivitelline space of superovulated PV-Cre mice and pups were genotyped by qPCR (Table 1) to check for the presence and relative quantity of the transgene, according to the protocol described in Barde et al. (2011).

Mice showing consistent and robust expression of eGFP (Table 2) were mated with PV-Cre mice to establish genetically stable lines. Transgene-carrying mice in the offspring were identified based on eGFP expression of cells obtained by peritoneal lavage, using a protocol modified from Bot et al. (2003)). Briefly, mice were anesthetized with isoflurane and were injected in the peritoneal cavity with 3–5 ml of Ca^{2+}- and Mg^{2+}-free Dulbecco's PBS (Gibco, Basel, Switzerland) and peritoneal aspirates were collected. Mice were returned to their home cage and monitored until complete recovery to the awaken state. Peritoneal aspirates (200 μl) were then cultured in DMEM and green fluorescence was monitored by the Incucyte Live Cell Imaging System.

IPTG was applied i.p. to eGFP^{+} mice from the F2 and F3 generations at a dose of 1 mg in 200 μl (three injections, one every 3 days; (modified from Grespi, Ottina, Yannoutsos, Geley, & Villunger, 2011). Following treatment, mice were killed via cervical dislocation and brains were harvested, dissected and stored at −80°C until use.

TABLE 1 qPCR primers for the genotyping of transgenic animals obtained by lentiviral-mediated transgenesis

Sequence detected	Primer pairs	Primer sequence
WPRE	WPRE _forward	GGCACTGACAATTCCGTGGT
	WPRE_ reverse	AGGGACGTAGCAGAAGGACG
TITIN	Titin_ forward	AAAACGAGCAGTGACGTGAGC
	Titin_ reverse	TTCAGTCATGCTGCTAGCGC
eGFP	eGFP_ forward	ACG TAA ACG GCC ACA AGT TC
	eGFP_ reverse	AAG TCG TGC TGC TTC ATG TG

TABLE 2 Transgenic founder mice (F0) from lentiviral-mediated transgenesis

Strain/animal ID	eGFP$^+$ cells	Copy number	Strain/animal ID	eGFP$^+$ cells	Copy number
B6PV-Cre shPV22_ 277	24.7	5.2	B6PV-Cre shTurboGFP_181	0.2	3.5
B6 PV-Cre shPV22_283	2.6	>10	**B6PV-Cre shTurboGFP_236**	0.6	>10
B6PV-Cre shPV22_284	13.1	>10	B6PV-Cre shTurboGFP_243	4.2	0.1
B6PV-Cre shPV22_491	0.2	>10	B6PV-Cre shTurboGFP_522	0.1	2.0
B6PV-Cre shPV22_509	0.1	6.0	B6PV-Cre shTurboGFP_521	0.1	>10
B6PV-Cre shPV22_494	13.5	>10	B6PV-Cre shTurboGFP_524	5.3	1.3

Note: The F1 generation from the founders (bold) was selected for further breeding.

2.4 | Immunohistochemistry and western blot analysis

Mice were perfused to determine the distribution of the constitutive expression of the transgene (eGFP) by immunofluorescence staining on brain sections. Mice were deeply anesthetized (Esconarkon (1 ml/kg, diluted with NaCl 0.9%), Streuli Pharma AG, Uznach, Switzerland) and perfused with 0.9% saline solution followed by 4% PFA. Brains were removed and post-fixed for 24 hr in 4% PFA before cryopreservation in 30% sucrose-TBS at 4°C. Coronal sections (40 μm) were cut using a freezing microtome (Frigomobil, Reichert-Jung, Vienna, Austria) and first incubated with TBS 0.1 M, pH 7.6, plus 0.4% Triton X-100 and 10% newborn calf serum (NBS) for 1 hr at room temperature, then washed three times with TBS 0.1 M, and incubated with PV antibody (guinea pig anti-PV72, 1:1000; Swant, Marly, Switzerland), rabbit anti-GFP (1:1000, Molecular Probes; Thermo Fisher Scientific, Reinach, Switzerland), guinea pig anti-S100β (1:500; Synaptic Systems, Gottingen, Germany) or mouse anti-NeuN (Abcam, Ab177487, 1:1000) in TBS 0.1 M overnight at 4°C. Sections were washed once with TBS, then twice with Tris-HCl, pH 8.2, and incubated protected from light at room temperature with species-specific fluorophore-conjugated secondary antibodies: guinea pig Cy3-conjugated antibody, rabbit Alexa488-conjugated antibody and mouse Cy3-conjugated antibody (1:200 dilution; Milan Analytic AG, Switzerland) in Tris-HCl. Nuclei of fixed cells were stained with DAPI (1:500 dilution; LuBio Science GmbH, Luzern, Switzerland) in 0.1 M PBS, pH 7.3. After rinsing, slides were coverslipped with Hydromount (National Diagnostics, Atlanta, GA, USA). Western blots were performed as described before (Filice, Vörckel, Sungur, Wöhr, & Schwaller, 2016). Protein extracts (50 μg) were loaded on SDS-PAGE gels (12.5% polyacrylamide) and transferred onto nitrocellulose membranes (MS solution; Chemie Brunschwig, Basel, Switzerland). The membranes were then blocked in 5% non-fat milk in TBS-T for 60 min at room temperature and incubated with primary antibody rabbit anti-PV25 (Swant) diluted 1:10,000 in 2% non-fat milk in TBS-T overnight at 4°C. Membranes were washed three times in TBS-T and incubated for 1 hr with secondary antibody (goat anti-rabbit IgG HRP conjugated; Sigma-Aldrich) diluted at 1:10,000 in TBS-T. Finally, membranes were repeatedly rinsed in TBS-T and developed using ECL (Merck Millipore, Schaffhausen, Switzerland). Bands visualized by ECL were quantified using Alpha VIEW SA software (CA, USA). The levels of PV signals were normalized using the integral of total protein signals per sample of the Ponceau Red-stained membranes as described before (Gilda & Gomes, 2013). Statistical analysis was performed using GraphPad Prism 7 software (San Diego, CA, USA), applying Student's *t* test to compare protein levels between control and IPTG-treated mice. p-Values < 0.05 were considered statistically significant.

3 | RESULTS

3.1 | Generation and characterization of plasmids allowing for modulation of PV expression

We aimed to generate a transgenic mouse model, in which the *Pvalb* gene can be regulated in an inducible and reversible manner. For this, a commercially available and validated shRNA against mouse *Pvalb* was cloned into a plasmid consisting of an IPTG-inducible lentiviral backbone engineered to contain: (a) a reporter cassette encoding eGFP independently translated through the commonly used human 3-phosphoglycerate kinase (hPGK) promoter, (b) a LacI repressor and (c) a modified human U6 shRNA promoter with LacO (operator) sequences (Figure 1). The shPvalb sequence is complementary to the region from 156 to 174 of the CDS of the mouse *Pvalb* sequence (NM_001330686.1; CDS: 93-425). To determine the efficiency of the IPTG-inducible system in vitro, we stably overexpressed PV in RN5 cells. RN5-PV cells were then transfected either with the inducible 3X-LacO-eGFP-shPV22 (hereafter shPV22) or 3X-LacO-eGFP-shTurboGFP plasmids (control vector, hereafter shTurboGFP). In the transfected cells, eGFP expression was detectable after 24 hr (Figure 2a). Cells were then treated with IPTG for 5 days; such a treatment had no effect on PV protein expression levels in RN5-PV cells transfected with the plasmid coding for

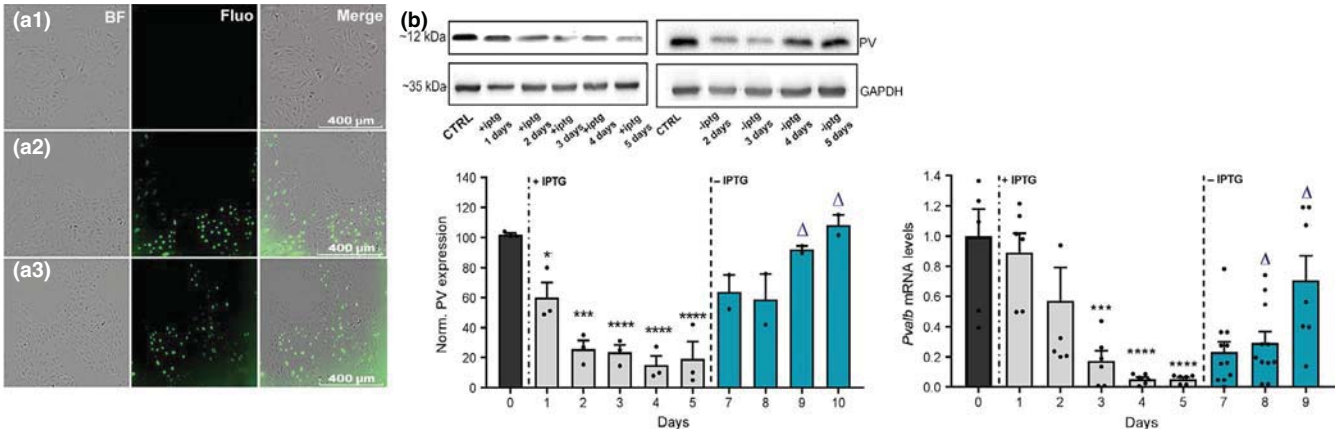

FIGURE 2 (a) Murine RN5-PV cells transfected with LV carrying shRNA (*shPV22* or *shTurboGFP*) express the eGFP reporter protein. (a1) control RN5-PV cells (a2) RN5-PV cells transduced with LV containing the *shPV22* sequences. (a3) RN5-PV cells transduced with LV containing the *shTurboGFP* sequences. In all cases a brightfield (BF), a fluorescence (Fluo) and the merged (Merge) images are shown. (b) western blot analysis (left) of PV protein levels in cultured RN5-PV cells (control (CTRL) defined as 100%; black bar) co-transfected with the inducible shPV22 cultured in the presence of 1 mM IPTG (gray bars) and after removal of IPTG (blue bars). GAPDH western blot signals were used as loading controls and for normalization. In parallel, relative *Pvalb* mRNA levels (right) in LV-transduced RN5-PV cells were determined by RT-qPCR. The *Pvalb* mRNA level of control RN5-PV cells was defined as 1.0. 18S rRNA RT-qPCR signals were used for normalization. *, *** and **** indicates significance ($p < 0.05$, $p < 0.001$ and $p < 0.0001$, respectively) versus non-IPTG-treated. Δ indicates significance ($p < 0.05$) versus IPTG-treated day 5. eGFP, enhanced green fluorescent protein. [Colour figure can be viewed at wileyonlinelibrary.com]

shTurboGFP (Supporting Information Figure S1, upper part). Quantification of PV signals with GAPDH serving as normalization signal revealed no significant changes in PV expression levels (Supporting Information Figure S1, lower part); also, eGFP fluorescence was not affected by the induction of the shTurboGFP (not shown), as the target sequence of the latter is not complementary to the eGFP sequence of the LV construct used for transgenesis.

While eGFP expression remained stable also in RN5-PV cells transfected with the shPV22, IPTG led to a time-dependent decrease in PV protein levels; a significant decrease by ~80% was observed from day 2 on, and remained similar until day 5 under continuous IPTG treatment (Figure 2b, gray bars), as evidenced by western blot analysis. When cells were subsequently grown in medium without IPTG, PV levels recovered to ~50% 2 days later (day 7) and to PV levels prior to IPTG induction from day 9 on (Figure 2b, blue bars). The time course of changes in *Pvalb* mRNA levels determined by RT-qPCR showed an almost identical profile: a rapid decrease to ~5% of control RN5-PV in the presence of IPTG at day 4, followed by a rather quick recovery after IPTG removal (Figure 2b, right part).

3.2 | Production of transgenic mice with adjustable PV expression

Having verified the proper functioning of the lentiviral shRNA vectors in vitro, transgenic mice were produced by lentiviral transgenesis in vivo that is, injection of the vector-containing (shPV22 and shTurboGFP) LV beneath the zona pellucida of fertilized oocytes of PV-Cre mice (Barde et al., 2011). The selection of PV-Cre mice instead of wild-type C57Bl/6J mice allows crossing these mice at later stages with transgenic lines with floxed genes, to enable specific targeting of selected genes in Pvalb neurons. The copy number of the transgene, as well as the percentage of eGFP-positive ($eGFP^+$) cells was determined in founder mice (F0) as follows: 100 µl of blood were collected from the tail vein of each transgenic animal; leucocytes were isolated and analyzed by flow cytometry to measure the percentage of $eGFP^+$ cells. The number of integrated transgene copies was analyzed by qPCR using genomic DNA from white blood cells, using the sequence of the woodchuck hepatitis virus post-transcriptional response element (WPRE), present in the lentiviral plasmid. For normalization, sequences of the mouse *Ttn* gene coding for titin, known to be present at two copies per genome (two alleles), were amplified (for a detailed protocol see Barde et al., 2011). eGFP levels varied considerably between founders (Table 2), likely due to positioning effects of the transgene and the copy number of the integrated plasmid (Wilson, 1990). Within the group of transgene-expressing F0 mice, we chose the ones showing highest $eGFP^+$ expression for further breeding. Six founders (four for shPV22 and two for shTurboGFP, see Table 2) were subsequently used to establish transgenic lines by breeding them with PV-Cre mice. Three lines (#277 and #284 for shPV22; #236 for shTurboGFP) were further bred to PV-Cre mice until having offspring of the third generation (F3), as transgene inheritance is generally unstable in early generations (Morton, Chaston, Baillie, Hill, & Matthaei, 2014). The

identification of mice carrying the transgene in these generations was based on the visualization of eGFP$^+$ cells (using the Incucyte Imaging system) from peritoneal aspirates. On average, half of the progenies of ≥F3 generations were positive for eGFP, in line with Mendelian inheritance given that the transgene is integrated at a single locus.

3.3 | Ex vivo experiments with primary fibroblasts from transgenic mice

As the hPGK promoter driving eGFP expression and the hU6 2xLacO promoter driving shRNA (*Pvalb* or *TurboGFP*) function independently (Stewart et al., 2003), the presence of eGFP is not directly correlated with the functionality/levels of the shRNA. It is known that transgene expression in the offspring of transgenic breeders may be decreased or prevented by positional effects and/or DNA methylation mechanisms (Curradi, Izzo, Badaracco, & Landsberger, 2002; Whitelaw et al., 2001). We assessed the absence of in vivo silencing of the shPV22 in ex vivo isolated lung fibroblasts from transgenic offspring. eGFP fluorescence was detected in the nucleus of cultured fibroblasts after 48 hr (data not shown), indicating that the hPGK promoter driving the reporter cassette was not silenced in vivo. To demonstrate the functionality of *Pvalb* shRNA in fibroblasts from transgenic mice, we infected these cells with a LV leading to the ectopic expression of either PV (lentiviral construct Phage-PV) or a fusion protein consisting of the monomeric red fluorescence protein mRFP as the N-terminal part followed by the amino acids of PV (Phage-mRFP-PV). Expression levels of mRFP-PV were directly monitored by fluorescence microscopy. In the absence of IPTG, essentially all fibroblasts showed red fluorescence to variable degrees (Figure 3a, top right). After IPTG treatment for 1 week, the red fluorescence was considerably decreased in most cells, with only few cells still showing strong fluorescence (Figure 3a, lower right). On western blots, protein extracts from LV-mRFP-PV fibroblasts maintained in the absence of IPTG showed a strong signal at approximately 40 kDa, the expected size of the mRFP-PV fusion protein. The signal was significantly reduced (>80% downregulation) in extracts from cultured fibroblasts subjected to IPTG treatment (Figure 3b, red bars). The lower band slightly below 40 kDa is likely a degradation product of mRFP-PV or due to a pre-terminal stop. Essentially identical results were obtained in cells infected with LV-PV; Figure 3b, black bars). Thus, as in RN5-PV cells, the entire transgene (eGFP expression + shPV22 production) was functional also in isolated primary fibroblasts from transgenic mice.

3.4 | In vivo experiments with transgenic mice

Due to the ubiquitous expression of the PGK promoter, the eGFP reporter should be (theoretically) expressed in all the

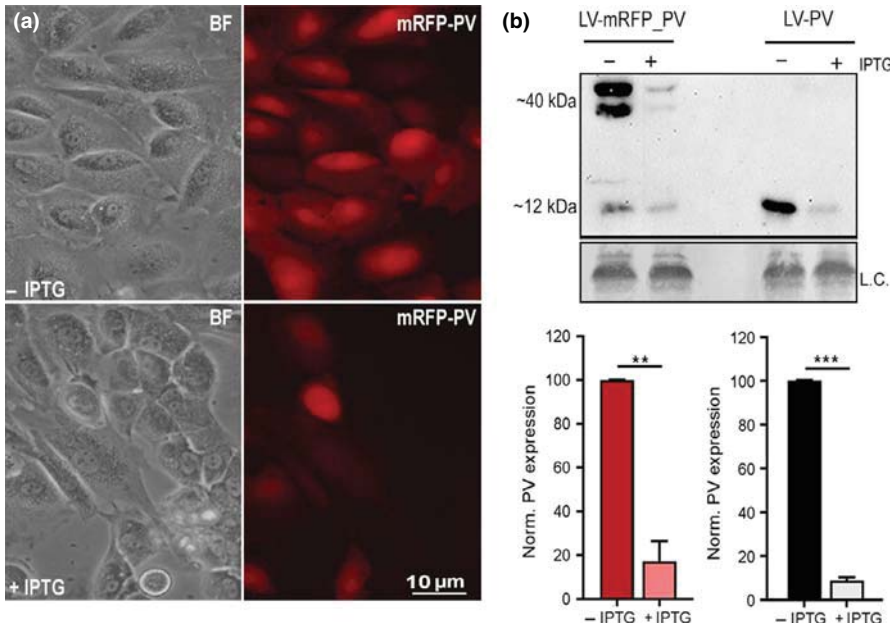

FIGURE 3 Ex vivo experiments with isolated primary lung fibroblasts from shPV22 #284_F2 mice. (a) Left panels: Brightfield (BF) images of fibroblasts transfected with the LV expressing the fusion protein mRFP-PV. Right panels: Fluorescence images of the same cells. Fluorescent intensity decreases upon IPTG (1 mM) treatment for 1 week, indicating a downregulation of mRFP-PV levels (lower image). (b) Upper panel: western blot analysis of mRFP-PV and PV downregulation in isolated fibroblasts expressing mRFP-PV (left lanes) or PV (right lanes), before (−) and after (+) IPTG treatment. The intensity of the Ponceau Red-stained membrane was used as loading control (L.C.). Lower part: Quantification of the western blot signals above and one additional blot. ** and *** indicates significance ($p < 0.01$ and $p < 0.001$, respectively) versus non-IPTG-treated (−) cells. [Colour figure can be viewed at wileyonlinelibrary.com]

cells of transgenic mice; however, its expression levels might vary depending on the activity of the promoter in various cell types and tissues. In order to get insight on the spatial and cellular distribution of the transgene, or more precisely, on the activity of the hPGK promoter driving eGFP expression, we performed immunostaining on brain slices using antibodies against eGFP. $eGFP^+$ cells were detected throughout the brain, in both glial ($S100\beta^+$) and neuronal ($NeuN^+$) cells, as shown in Supporting Information Figure S2. As we were primarily interested whether the transgene is expressed in the population of Pvalb neurons, where we intended to downregulate *Pvalb* mRNA and thus PV expression, we checked to what extent $eGFP^+$ cells overlapped with PV^+ neurons. Double-stained cells (PV^+/$eGFP^+$) were observed in multiple brain areas, such as cortex, cerebellum, hippocampus, thalamus and striatum. In particular, a strong co-localization of eGFP and PV was observed in the cerebellum, cortex and thalamus (Figure 4a,c,e), while a weaker co-staining was present in the striatum and hippocampus (Figure 4b,d).

Next, we evaluated the efficiency of PV downregulation after IPTG administration in transgenic mice in vivo. Due to the highly heterogeneous expression of PV in different brain regions, we measured PV levels in dissected regions of the mouse brain, in order to obtain more accurate information on the extent of PV downregulation. The following regions were dissected and analyzed separately: cerebellum, cortex, hippocampus and thalamus. Comparison of IPTG-treated (three i.p. injections at intervals of 3 days at days PND18, 21 and 24, dissection at day 25) transgenic mice with sham-treated (saline) controls showed efficient downregulation of PV by ~50%–60% in the cerebellum, cortex, hippocampus and thalamus (Figure 4f), to similar levels as present in PV heterozygous ($PV^{+/-}$) mice (see Schwaller et al., 2004).

To further verify the specificity of our approach in vivo, transgenic mice carrying the shTurboGFP transgene were treated with IPTG. Brains were only separated into forebrain and cerebellum. In protein extracts from both regions, addition of IPTG in vivo had no effect on PV expression levels determined at PND25 (Supporting Information Figure S3).

Finally to test the reversibility of the inducible system in vivo, mice treated with IPTG were then maintained for a period of 3 weeks without IPTG; PV levels returned to basal (initial) levels (Figure 4g), indicating that PV levels can be manipulated in vivo in an inducible and reversible manner.

3.5 | Immunohistochemical analysis of PV expression in control and IPTG-treated transgenic shPV22 mice

After having established IPTG-induced downregulation of PV and *Pvalb* mRNA expression in fibroblasts (Figure 3) and of PV protein levels in various brain regions from transgenic mice (Figure 4), we investigated the distribution of PV^+ neurons in the brain of transgenic mice with a focus on the cortex, striatum and reticular thalamic nucleus (RTN). The former two regions were selected based on the reported decrease in PV expression in ASD mouse models including $PV^{+/-}$, $Shank1^{-/-}$, $Shank3B^{-/-}$ and $Cntnap2^{-/-}$ and in utero VPA-exposed mice (Filice et al., 2016; Lauber, Filice, & Schwaller, 2016, 2018). In control (untreated) transgenic mice, the typical laminar distribution of PV^+ cells, as well as the relative density of PV^+ neurons in the different cortical layers was observed (Figure 5); the staining pattern was indistinguishable from the one reported before in many studies (e.g., fig. 2 in Schwaller et al., 2004). The density of PV^+ neurons in the striatum was clearly lower than in the cortex with a higher proportion of PV^+ neurons in the lateral part compared to the medial part, as reported before (e.g., fig. 1 in Russo, Nieus, Maggi, & Taverna, 2013). In the IPTG-treated transgenic mice, no evident changes in the distribution of PV^+ neurons were observed, however, staining intensities of PV^+ cells were globally decreased. A comparison of brain sections from a $PV^{+/-}$ mouse, where PV levels are constitutively decreased by ~50% in comparison to a WT ($PV^{+/+}$) mouse (Schwaller et al., 2004), with a shPV22 transgenic mouse treated with IPTG from PND 18–24 and killed at PND 25, revealed a very similar

FIGURE 4 (a–e) $eGFP^+$ (green) and PV^+ (purple) cell distribution in different brain regions of shPV22 mice (line #277). (a) Cerebellum: eGFP is detected in the molecular layer (ML), Purkinje cell layer (P) and the granule cell layer (GL). (b) Hippocampus: fluorescent cells are visible in the dentate gyrus (DG), as well as in the hilus (h). m, stratum moleculare; g, stratum granulosum. (c) Neocortex: $eGFP^+$ cells are visible throughout all layers (I to VI). (d) Striatum and (e) Reticular thalamic nucleus (RTN): $eGFP^+$ cells are detected in all regions. For all brain regions, co-immunostaining with PV (purple) and the merged image (Merge) is shown. TH, thalamus; LVe, lateral ventricle; int, internal capsulae. (f) Western blot analysis (upper part) and quantification of PV downregulation (lower part) after i.p. IPTG treatment at PND18, 21 and 24. Different brain regions were dissected at PND25. Dots represent values from three independent blots (each containing samples from six mice); *p*-values are indicated for the IPTG-mediated PV downregulation in the various regions. (g) Reversibility of PV expression in vivo. Forebrain western blot analysis of PV downregulation after IPTG i.p. injection from PND18-24, brain collection at PND25 (+IPTG) and 3 weeks after IPTG withdrawal (−IPTG). For the normalization of the western blot signal (left panel), the intensity of the Ponceau Red-stained membrane (L.C.) was used. Right panel: IPTG treatment reduces PV levels by approx. 50% (white bar). 3 weeks after IPTG removal PV levels return to the control (−IPTG) situation (green bar). ** indicates $p < 0.01$ NO IPTG versus IPTG-treated mice; Δ indicates significance ($p < 0.05$) for comparison of IPTG-treated versus IPTG withdrawal. eGFP, enhanced green fluorescent protein. [Colour figure can be viewed at wileyonlinelibrary.com]

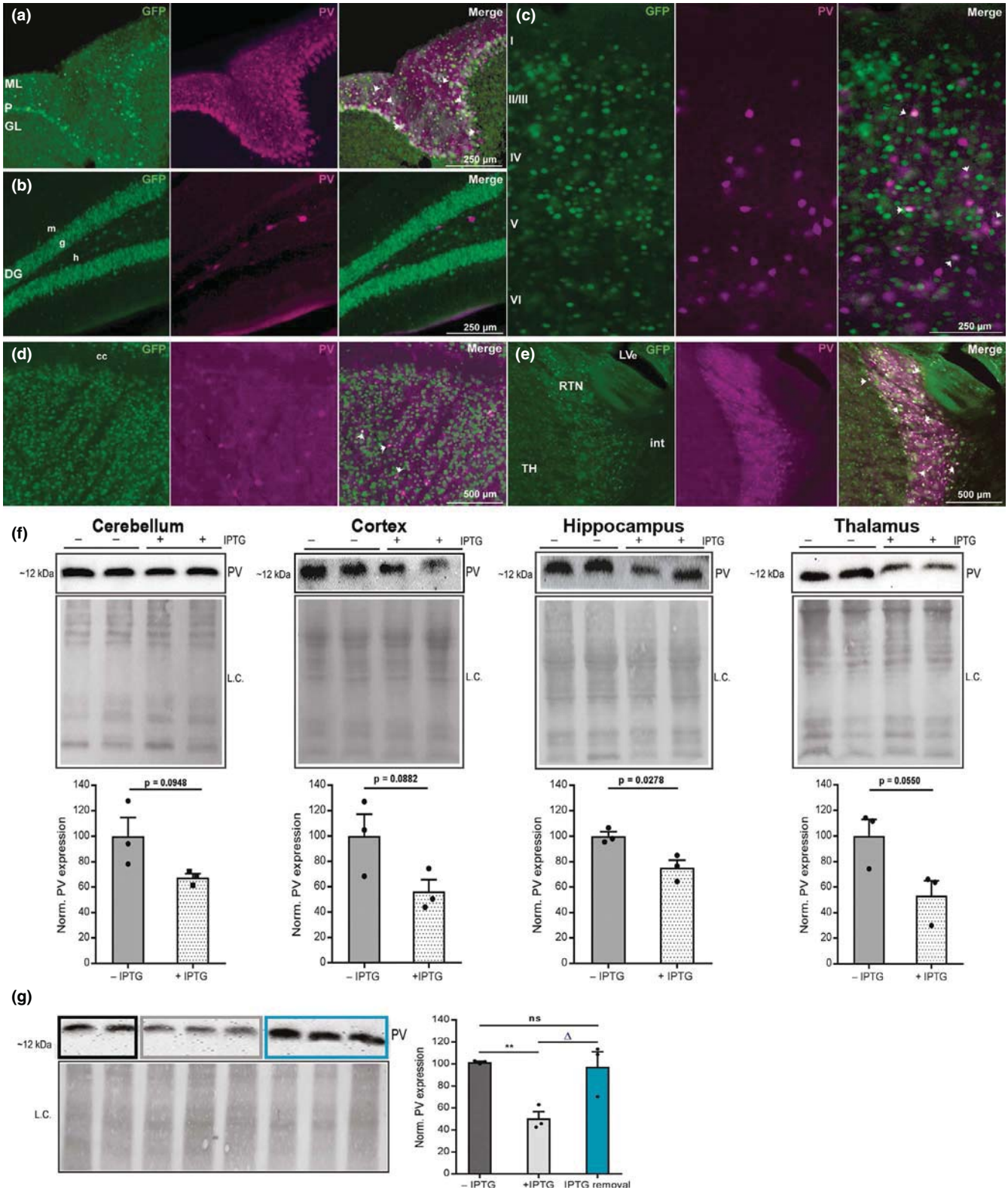

staining pattern (Figure 5). While the decrease in staining intensity of PV^+ neurons was highly evident in cortical and striatal PV^+ neurons, the effect was less pronounced in the RTN, possibly due to the very high PV expression levels in those neurons. Yet globally, PV immunostaining results indicate that the distribution of PV^+ neurons is not altered in the transgenic mice and, moreover, that PV downregulation by IPTG-induced *shPV22* synthesis is rather homogenous in PV^+ neurons throughout the brain and thus closely resembling the state prevailing in $PV^{+/-}$ mice. As expected, we found no indication of ectopic PV expression in the transgenic mice and also no brain regions,

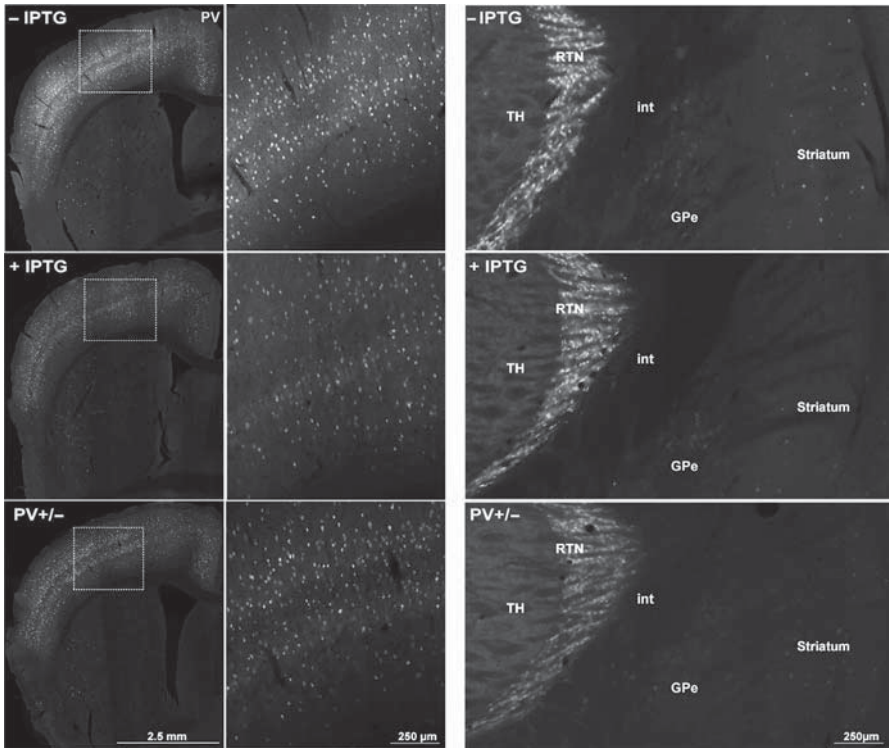

FIGURE 5 PV immunofluorescence staining of cortex (left panel), reticular thalamic nucleus (RTN) and striatum (right panel) of an untreated (-IPTG) shPV22 mouse (line #277), a shPV22 transgenic mouse treated with IPTG (experimental conditions as shown in Figure 4) and a $PV^{+/-}$ mouse, the latter expressing approximately 50% of PV protein levels compared to $PV^{+/+}$ or untreated shPV22 mice. Cortex regions boxed with white lines are shown at higher magnification in the middle panel

where PV downregulation was over-proportionally strong, i.e., resulting in an apparent "loss" of PV^{+} neurons or vice versa, regions where staining intensities remained as high as in $PV^{+/+}$ mice. Thus, in all investigated aspects, PV expression levels and localization was principally identical in IPTG-treated transgenic mice and $PV^{+/-}$ mice.

4 | DISCUSSION

In the early 1980s, the generation of the first "transgenic mouse" by Brinster and Palmiter (reviewed in Hanahan, Wagner, & Palmiter, 2007), inaugurated a new era in many biological fields and provided a new methodology to model human diseases in an animal context. Up to date, several transgenic mouse lines targeting the *Pvalb* gene (www.jax.org, Table 3) have been generated, resulting in animals with abolished gene function (knockout mice) or expressing Cre-recombinase/channelrhodopsins/reporter fluorescent proteins (GFP, tdTomato) selectively in Pvalb neurons. Nevertheless, none of these models allows for temporal modulation of *Pvalb*/PV expression.

Due to the implication of Pvalb neurons in neurodevelopmental diseases, such as ASD and schizophrenia, (Marin, 2012; Volk et al., 2012), we have developed, combining lentiviral-mediated transgenesis and RNA interference (RNAi), a new reversible and inducible system for *Pvalb* gene downregulation in mice, where the temporal control of *Pvalb* gene expression (switch on/off) is tightly regulated by the presence/absence of IPTG and, moreover, allows to modulate PV protein expression (in a reversible way) over a long period of time.

Several regulatable systems have been developed in the last 30 years for transgene expression often derived from prokaryotic organisms (reviewed in Yamamoto, Hen, & Dauer, 2001; Matthaei, 2007). The system most widely applied is the tetracycline response system (tet on/off), where a tetracycline-responsive transactivator protein tTa (tet-off) or a reverse transactivator (rTa; tet-on) is expressed in transgenic mice, sometimes also under the control of a tissue-specific promoter. Of note, tetracycline (T_c) and the more often used doxycycline (dox) are antibiotics; side effects in humans including diarrhea, nausea and vomiting are well known, the former likely caused by the effect of the antibiotics on the intestinal microbiota. However, the effects of long-term exposure and/or of prenatal T_c exposure in mice are still uncertain. T_c is also stored in bones and thus slowly cleared from the body of treated mice. For these reasons, an alternative system based on the *lac* operon of *E. coli* was developed and successfully tested in mice (Cronin, Gluba, & Scrable, 2001). In this system, transgene expression is induced by the lactose analog IPTG, which can be added to the drinking water. IPTG is well tolerated also after long exposure with no noticeable side effects (Cronin et al., 2001). IPTG is taken up rapidly by all tissues including the endothelium (Morton et al., 2014) and brain tissue, as it crosses the blood–brain barrier and is highly stable intracellularly (Wyborski & Short, 1991). As with

TABLE 3 Transgenic mouse lines targeting the *Pvalb* gene

STRAIN	Description
B6;129P2-Pvalbtm1(cre)Arbr/J	PV-Cre knock-in mice express Cre recombinase in parvalbumin-expressing neurons, such as interneurons in the brain and proprioceptive afferent sensory neurons
B6.129P2-Pvalbtm1Swal/J	Parvalbumin knockout mice exhibit a prolonged contraction–relaxation cycle in fast-twitch muscle, as well as multiple behavioral phenotypes associated with autism spectrum disorder (ASD)
B6.Cg-Pvalbtm1.1(cre/ERT2) Hze/J	Pvalb-2A-CreERT2-D mice have Cre-ERT2 fusion gene expression directed to Pvalb-expressing cells by the endogenous promoter/enhancer elements of the *Pvalb* locus. These mice serve as a "Cre-lox tool" that allows inducible Cre expression of genes in Pvalb-expressing cells/tissues
C57BL/6N-Tg(Pvalb-tdTomato/RNAi:Gad1)3Mirn/J	The Pvalb-tdTomato-miGAD67 line 3 BAC transgenic mouse line is a hybrid reporter/miRNA knockdown model, where parvalbumin interneuron expression of a synthetic *Gad1* miRNA precursor results in *Gad1* transcript downregulation (silencing of GAD1 expression) via endogenous miRNA processing mechanisms. These mice may be useful in studying Pvalb GABAergic interneurons in behavioral and molecular processes, as well as cell-type specific GABAergic disturbances in manifestations of schizophrenia
B6;SJL-Tg(Pvalb-COP4*H134R/EYFP)15Gfng/J	Prv-mhChR2-YFP BAC transgenic mice express an improved channelrhodopsin-2/EYFP fusion protein (mhChR2::YFP) directed to neuronal populations by the mouse *Pvalb* promoter/enhancer on the BAC transgene. Illuminating mhChR2-expressing neurons with blue light (450–490 nm) leads to rapid and reversible photostimulation of action potential firing/neural activity in these cells. These transgenic mice can be used in optogenetic studies for in vivo control of motor behavior by addition or removal of blue light
B6(Cg)-Pvalbtm1(cre/ERT2) Zjh/J	The PV-CreERT2 knock-in allele in these mice both abolishes *Pvalb* gene function and expresses the CreERT2 fusion protein directed to Pvalb neurons in the neocortex and cerebellum by the endogenous *Pvalb* promoter/enhancer elements

all systemic application methods (oral, i.p.), it is difficult to estimate the real IPTG concentration in the extracellular space surrounding the Pvalb neurons. It is very likely to be lower than in the medium (1 mM IPTG) to which RN5-PV cells were exposed in vitro. The literature concerning putative adverse systemic effects of IPTG is still sparse; higher systemic IPTG application (concentration/frequency) than that used in this study may be necessary, if a more efficient knockdown of PV is required for particular in vivo experiments.

We first confirmed the inducing ability and reversibility of *Pvalb* knockdown in vitro; in cell models, that is, PV-expressing RN5 cells and isolated primary fibroblasts from transgenic mice, IPTG (at a concentration of 1 mM) efficiently induced *shPV22* expression and consequently the downregulation of PV expression to ≤20% of the initial levels. The degree of inducible downregulation was similar to levels obtained by a constitutive lentiviral shRNA against PV used previously in MDCK cells (Henzi & Schwaller, 2015). Removal of IPTG completely restored the initial situation in about 5 days, confirming the reversibility of our system.

We next generated the transgenic mouse line via lentiviral-mediated transgenesis. Overall, shPV22-PV-Cre mice (lines #277 and #284) as described here, bred normally and showed no changes in gross morphological aspects and also no obvious behavioral phenotype. That is, under standard housing conditions, no phenotype was discernible, even to experienced animal caretakers. The presence of the *eGFP* cassette in the vector allowed for monitoring transgene expression in the brain: $eGFP^+$ cells were detected principally in neuronal

cells, with very limited expression in other cell types (e.g., glial cells); this is consistent with the eGFP reporter being driven by the hPGK promoter (Naldini et al., 1996). To confirm that in the selected transgenic lines, PV downregulation is achievable, we treated the animals with IPTG. Intraperitoneal IPTG administration at days PND18, 21 and 24 induced the expression of the *shPV22*, which eventually led to an efficient downregulation of PV protein expression levels detected at PND25. Of importance for future behavioral experiments, PV levels after IPTG-mediated downregulation, as well as the distribution and staining intensities of PV^{+} cells were similar to those observed in well-known ASD mouse models such as $Shank3B^{-/-}$, VPA-exposed, $Cntnap2^{-/-}$ and $PV^{+/-}$ mice (~50% of WT (see Schwaller et al., 2004; Wöhr et al., 2015; Filice et al., 2016; Lauber et al., 2016, 2018)). Moreover, strongly in support of the importance of the reversibility of shRNA-mediated PV downregulation, we had shown that the ASD-related phenotype in $PV^{+/-}$ mice (Wöhr et al., 2015) was attenuated following the upregulation of PV levels via estradiol (E2) administration during early postnatal development (Filice, Lauber, Vorckel, Wöhr, & Schwaller, 2018). However, reduced expression of PV has been reported not only in postmortem brains from patients suffering from ASD, but also in brains from schizophrenic individuals (Gonzalez-Burgos, Cho, & Lewis, 2015; Hashemi, Ariza, Rogers, Noctor, & Martinez-Cerdeno, 2017). Furthermore, alterations of Pvalb neuron circuitry are recapitulated in animal models of such psychiatric disorders (Gandal, Nesbitt, McCurdy, & Alter, 2012).

Being well established that ASD and schizophrenia have different temporal trajectories, that is, later onset in schizophrenia (DeLisi, 1992; Minshew, 1996) and that PV downregulation is common to both, the validation in this study of this new transgenic line makes these mice particularly interesting for further investigation of the temporal profile of PV expression, that is, at which time point PV downregulation might lead to an ASD-like phenotype, rather than a schizophrenic-like phenotype.

The mouse model allows for a transient and inducible silencing/downregulation of PV during particular neurodevelopmental periods, including the "critical" period, in which the formation of neuronal circuits in the brain occurs (Hensch, 2005). We hypothesize that these newly generated mouse lines may provide a powerful tool to get further insights into the mechanisms of diseases (ASD, schizophrenia) characterized by dysfunctions of Pvalb neurons and Pvalb neuron circuits and possibly might pave the way for testing new therapies in such neurodevelopmental diseases.

ACKNOWLEDGEMENTS

This project was supported by grants from the Swiss National Science Foundation (SNSF # 310030_155952/1) and Novartis Foundation for medical-biological research (#16C172). The authors wish to thank Simone Eichenberger for the maintenance of the mouse facility.

CONFLICT OF INTEREST

The authors declare no competing financial interests.

DATA ACCESSIBILITY

Data are available upon request from the corresponding author.

AUTHOR CONTRIBUTIONS

FF carried out all the experiments, collected the data, participated in setting up the experiments and analyzed the data. WB participated in setting up the experiments and reviewing the manuscript. EL helped performing western blot experiments and reviewing the manuscript. BS conceived the study and supervised and assisted with data analysis. FF and BS wrote the paper. All of the authors read and endorsed the final version of the manuscript.

ORCID

Beat Schwaller https://orcid.org/0000-0002-8277-7555

REFERENCES

Barde, I., Salmon, P., & Trono, D. (2010). Production and titration of lentiviral vectors. *Current Protocols in Neuroscience*, *Chapter 4*, Unit 4.21.1–4.21.23.

Barde, I., Verp, S., Offner, S., & Trono, D. (2011). Lentiviral vector mediated transgenesis. *Current Protocols in Mouse Biology*, *1*, 169–184.

Blum, W., Pecze, L., Felley-Bosco, E., Worthmuller-Rodriguez, J., Wu, L., Vrugt, B., … Schwaller, B. (2015). Establishment of immortalized murine mesothelial cells and a novel mesothelioma cell line. In vitro *cellular & developmental biology*. *Animal*, *51*, 714–721.

Bot, J., Whitaker, D., Vivian, J., Lake, R., Yao, V., & McCauley, R. (2003). Culturing mouse peritoneal mesothelial cells. *Pathology, Research and Practice*, *199*, 341–344. https://doi.org/10.1078/0344-0338-00427

Campbell, R. E., Tour, O., Palmer, A. E., Steinbach, P. A., Baird, G. S., Zacharias, D. A., & Tsien, R. Y. (2002). A monomeric red fluorescent protein. *Proceedings of the National Academy of Sciences of the United States of America*, *99*, 7877–7882. https://doi.org/10.1073/pnas.082243699

Cronin, C., Gluba, W., & Scrable, H. (2001). The lac operator-repressor system is functional in the mouse. *Genes & Development*, *15*, 1506–1517. https://doi.org/10.1101/gad.892001

Curradi, M., Izzo, A., Badaracco, G., & Landsberger, N. (2002). Molecular mechanisms of gene silencing mediated by DNA methylation. *Molecular and Cellular Biology*, *22*, 3157–3173. https://doi.org/10.1128/MCB.22.9.3157-3173.2002

D'Astolfo, D. S., Pagliero, R. J., Pras, A., Karthaus, W. R., Clevers, H., Prasad, V., … Geijsen, N. (2015). Efficient intracellular delivery of native proteins. *Cell*, *161*, 674–690. https://doi.org/10.1016/j.cell.2015.03.028

DeLisi, L. E. (1992). The significance of age of onset for schizophrenia. *Schizophrenia Bulletin*, *18*, 209–215. https://doi.org/10.1093/schbul/18.2.209

D'Orlando, C., Fellay, B., Schwaller, B., Salicio, V., Bloc, A., Gotzos, V., & Celio, M. R. (2001). Calretinin and calbindin D-28k delay the onset of cell death after excitotoxic stimulation in transfected P19 cells. *Brain Research*, *909*, 145–158. https://doi.org/10.1016/S0006-8993(01)02671-3

Ferguson, B. R., & Gao, W. J. (2018). PV interneurons: Critical regulators of E/I balance for prefrontal cortex-dependent behavior and psychiatric disorders. *Frontiers in Neural Circuits*, *12*, 37. https://doi.org/10.3389/fncir.2018.00037

Filice, F., Lauber, E., Vorckel, K. J., Wöhr, M., & Schwaller, B. (2018). 17-beta estradiol increases parvalbumin levels in Pvalb heterozygous mice and attenuates behavioral phenotypes with relevance to autism core symptoms. *Molecular Autism*, *9*, 15. https://doi.org/10.1186/s13229-018-0199-3

Filice, F., Vörckel, K. J., Sungur, A. Ö., Wöhr, M., & Schwaller, B. (2016). Reduction in parvalbumin expression not loss of the parvalbumin-expressing GABA interneuron subpopulation in genetic parvalbumin and shank mouse models of autism. *Molecular Brain*, *9*, 10. https://doi.org/10.1186/s13041-016-0192-8

Gandal, M. J., Nesbitt, A. M., McCurdy, R. M., & Alter, M. D. (2012). Measuring the maturity of the fast-spiking interneuron transcriptional program in autism, schizophrenia, and bipolar disorder. *PLoS ONE*, *7*, e41215. https://doi.org/10.1371/journal.pone.0041215

Gilda, J. E., & Gomes, A. V. (2013). Stain-Free total protein staining is a superior loading control to beta-actin for Western blots. *Analytical Biochemistry*, *440*, 186–188. https://doi.org/10.1016/j.ab.2013.05.027

Gonzalez-Burgos, G., Cho, R. Y., & Lewis, D. A. (2015). Alterations in cortical network oscillations and parvalbumin neurons in schizophrenia. *Biological Psychiatry*, *77*, 1031–1040. https://doi.org/10.1016/j.biopsych.2015.03.010

Grespi, F., Ottina, E., Yannoutsos, N., Geley, S., & Villunger, A. (2011). Generation and evaluation of an IPTG-regulated version of Vav-gene promoter for mouse transgenesis. *PLoS ONE*, *6*, e18051. https://doi.org/10.1371/journal.pone.0018051

Hanahan, D., Wagner, E. F., & Palmiter, R. D. (2007). The origins of oncomice: A history of the first transgenic mice genetically engineered to develop cancer. *Genes & Development*, *21*, 2258–2270. https://doi.org/10.1101/gad.1583307

Hashemi, E., Ariza, J., Rogers, H., Noctor, S. C., & Martinez-Cerdeno, V. (2017). The number of parvalbumin-expressing interneurons is decreased in the medial prefrontal cortex in autism. *Cerebral Cortex*, *27*, 1931–1943.

Hensch, T. K. (2005). Critical period plasticity in local cortical circuits. *Nature Reviews. Neuroscience*, *6*, 877–888. https://doi.org/10.1038/nrn1787

Henzi, T., & Schwaller, B. (2015). Antagonistic regulation of parvalbumin expression and mitochondrial calcium handling capacity in renal epithelial cells. *PLoS ONE*, *10*, e0142005. https://doi.org/10.1371/journal.pone.0142005

Hippenmeyer, S., Vrieseling, E., Sigrist, M., Portmann, T., Laengle, C., Ladle, D. R., & Arber, S. (2005). A developmental switch in the response of DRG neurons to ETS transcription factor signaling. *PLoS Biology*, *3*, e159. https://doi.org/10.1371/journal.pbio.0030159

Jaenisch, R., & Mintz, B. (1974). Simian virus 40 DNA sequences in DNA of healthy adult mice derived from preimplantation blastocysts injected with viral DNA. *Proceedings of the National Academy of Sciences of the United States of America*, *71*, 1250–1254. https://doi.org/10.1073/pnas.71.4.1250

Kaiser, T., Ting, J. T., Monteiro, P., & Feng, G. (2016). Transgenic labeling of parvalbumin-expressing neurons with tdTomato. *Neuroscience*, *321*, 236–245. https://doi.org/10.1016/j.neuroscience.2015.08.036

Kutner, R. H., Zhang, X. Y., & Reiser, J. (2009). Production, concentration and titration of pseudotyped HIV-1-based lentiviral vectors. *Nature Protocols*, *4*, 495–505. https://doi.org/10.1038/nprot.2009.22

Lauber, E., Filice, F., & Schwaller, B. (2016). Prenatal valproate exposure differentially affects parvalbumin-expressing neurons and related circuits in the cortex and striatum of mice. *Frontiers in Molecular Neuroscience*, *9*, 150.

Lauber, E., Filice, F., & Schwaller, B. (2018). Dysregulation of parvalbumin expression in the Cntnap2$^{-/-}$ mouse model of autism spectrum disorder. *Frontiers in Molecular Neuroscience*, *11*, 262. https://doi.org/10.3389/fnmol.2018.00262

Marin, O. (2012). Interneuron dysfunction in psychiatric disorders. *Nature Reviews. Neuroscience*, *13*, 107–120. https://doi.org/10.1038/nrn3155

Matthaei, K. I. (2007). Genetically manipulated mice: A powerful tool with unsuspected caveats. *The Journal of Physiology*, *582*, 481–488. https://doi.org/10.1113/jphysiol.2007.134908

Meyer, A. H., Katona, I., Blatow, M., Rozov, A., & Monyer, H. (2002). In vivo labeling of parvalbumin-positive interneurons and analysis of electrical coupling in identified neurons. *The Journal of Neuroscience*, *22*, 7055–7064. https://doi.org/10.1523/JNEUROSCI.22-16-07055.2002

Minshew, N. J. (1996). Autism. In R. D. Adams & M. Victor (Eds.), *Principles of child neurology* (pp. 1713–1729). New York, NY: McGraw-Hill.

Morton, S. K., Chaston, D. J., Baillie, B. K., Hill, C. E., & Matthaei, K. I. (2014). Regulation of endothelial-specific transgene expression by the LacI repressor protein in vivo. *PLoS ONE*, *9*, e95980. https://doi.org/10.1371/journal.pone.0095980

Naldini, L., Blomer, U., Gallay, P., Ory, D., Mulligan, R., Gage, F. H., … Trono, D. (1996). In vivo gene delivery and stable transduction of nondividing cells by a lentiviral vector. *Science*, *272*, 263–267. https://doi.org/10.1126/science.272.5259.263

Russo, G., Nieus, T. R., Maggi, S., & Taverna, S. (2013). Dynamics of action potential firing in electrically connected striatal fast-spiking interneurons. *Frontiers in Cellular Neuroscience*, *7*, 209.

Schwaller, B., Dick, J., Dhoot, G., Carroll, S., Vrbova, G., Nicotera, P., … Celio, M. R. (1999). Prolonged contraction-relaxation cycle of fast-twitch muscles in parvalbumin knockout mice. *The American Journal of Physiology*, *276*, C395–C403. https://doi.org/10.1152/ajpcell.1999.276.2.C395

Schwaller, B., Tetko, I. V., Tandon, P., Silveira, D. C., Vreugdenhil, M., Henzi, T., … Villa, A. E. (2004). Parvalbumin deficiency affects network properties resulting in increased susceptibility to epileptic seizures. *Molecular and Cellular Neurosciences*, *25*, 650–663. https://doi.org/10.1016/j.mcn.2003.12.006

Seluanov, A., Vaidya, A., & Gorbunova, V. (2010). Establishing primary adult fibroblast cultures from rodents. *Journal of Visualized Experiments*, *44*, 2033. https://doi.org/10.3791/2033

Stewart, S. A., Dykxhoorn, D. M., Palliser, D., Mizuno, H., Yu, E. Y., An, D. S., … Novina, C. D. (2003). Lentivirus-delivered stable gene silencing by RNAi in primary cells. *RNA*, *9*, 493–501. https://doi.org/10.1261/rna.2192803

Volk, D. W., Matsubara, T., Li, S., Sengupta, E. J., Georgiev, D., Minabe, Y., … Lewis, D. A. (2012). Deficits in transcriptional regulators of cortical parvalbumin neurons in schizophrenia. *The American Journal of Psychiatry*, *169*, 1082–1091. https://doi.org/10.1176/appi.ajp.2012.12030305

Whitelaw, E., Sutherland, H., Kearns, M., Morgan, H., Weaving, L., & Garrick, D. (2001). Epigenetic effects on transgene expression. *Methods in Molecular Biology*, *158*, 351–368.

Wilson, C. (1990). Position effects on eukaryotic gene expression. *Annual Review of Cell Biology*, *6*, 697–714.

Wöhr, M., Orduz, D., Gregory, P., Moreno, H., Khan, U., Vorckel, K. J., … Schwaller, B. (2015). Lack of parvalbumin in mice leads to behavioral deficits relevant to all human autism core symptoms and related neural morphofunctional abnormalities. *Translational Psychiatry*, *5*, e525. https://doi.org/10.1038/tp.2015.19

Wyborski, D. L., & Short, J. M. (1991). Analysis of inducers of the *E. coli* lac repressor system in mammalian cells and whole animals. *Nucleic Acids Research*, *19*, 4647–4653. https://doi.org/10.1093/nar/19.17.4647

Yamamoto, A., Hen, R., & Dauer, W. T. (2001). The ons and offs of inducible transgenic technology: A review. *Neurobiology of Diseases*, *8*, 923–932. https://doi.org/10.1006/nbdi.2001.0452

Yue, F., Cheng, Y., Breschi, A., Vierstra, J., Wu, W., Ryba, T., … Pope, B. D. (2014). A comparative encyclopedia of DNA elements in the mouse genome. *Nature*, *515*, 355–364. https://doi.org/10.1038/nature13992